Geoderma 312 (2018) 151–158

Contents lists available at ScienceDirect

Geoderma

journal homepage: www.elsevier.com/locate/geoderma

Dissolved Si export: Impact of increased water fluxes through soil

Benedicta Ronchi[a,b,*], Alain Dassargues[c], Okke Batelaan[d]

[a] Institut Scientifique du Service Publique, Cellule Risques Sous-sol, Rue du Chéra 200, 4000 Liège, Belgium
[b] Katholieke Universiteit Leuven, Department of Earth and Environmental Sciences, Celestijnenlaan 200E, 3001 Leuven, Belgium
[c] Université de Liège, Hydrogeology and Environmental Geology, Department of Architecture, Geology, Environment, and Civil Engineering (ArGEnCo), B.52/3 Sart-Tilman, 4000 Liège, Belgium
[d] Flinders University, School of the Environment, GPO Box 2100, Adelaide, SA 5001, Australia

ARTICLE INFO

Handling Editor: Edward A. Nater

Keywords:
Kinetic dissolution
Biogenic silicon
Hydrus
Deforestation

ABSTRACT

Intense deforestation over large areas is an important component of global models which aim to quantify the transfer of terrestrial siliceous material from the continent to the coast. Hence, there is a need for improved understanding of land use impact on Si export. We present a model that simulates the kinetic dissolution of biogenic Si in a forest soil. A kinetic equation was calibrated based on leaching experiments of soil columns at constant water flux. The calibrated equation was then used to simulate the Si export from a forest soil under varying atmospheric conditions and provided realistic Si concentrations in soil water. The same model was used to simulate the impact of reduced evapotranspiration due to deforestation and consequently increased soil water fluxes on the Si export. Results showed that lower amounts of biogenic silicon dissolved and higher Si fluxes were released to the system once water flux increased. The use of the kinetic dissolution equation for biogenic Si improves our understanding and the modelling of the Si release from soils towards the hydrographic system.

1. Introduction

There is a growing interest in the impact of land management (forest, cropland) on Si export. Field observations show that rivers draining forests export larger Si fluxes than rivers draining agricultural areas (Struyf et al., 2010; Carey and Fulweiler, 2011). Higher Si fluxes exported from forests are explained by higher amount of biogenic Si (BSi) stored in forest soils compared to croplands (Clymans et al., 2011; Keller et al., 2012) as BSi dissolution is considered to control dissolved Si (DSi) concentrations in soil solutions (Farmer et al., 2005). Up to 40 years after deforestation, peaks of Si export have still been observed in rivers and were attributed to the erosion of the upper soil layer containing large BSi stocks. The high dissolved Si (DSi) export was attributed to the rapidly aggrading vegetation (Conley et al., 2008).

Previous studies generally addressed the behavior of dissolved Si (DSi) in rivers but less in soil water although Si is involved in several biochemical and geochemical subsurface processes, like chemical weathering, soil development, plant growth (Epstein, 1999; Raven, 2003). Moreover, ecosystems are often assumed at quasi steady-state, although seasonal variations in Si concentrations and water fluxes are typically observed in natural systems (e.g. Gérard et al., 2002; Fulweiler and Nixon, 2005; Clymans et al., 2013). Seasonal variation in rivers has been correlated to seasonal biological uptake (Carey and Fulweiler, 2013), but also to changes of pore-water supply to the river (Clymans et al., 2013).

Not much is known about the processes controlling Si dissolution in soils after land use changes. However, in the current context of intense deforestation over large areas of the African and South American continents, global models quantifying the transfer of terrestrial siliceous materials from the continent to the coast could be improved by developing understanding of land use impact on Si export (Tréguer and De La Rocha, 2013).

To identify the main processes controlling Si export in soils after deforestation, a model of Si dissolution is set up for a given environment with known geometry and time conditions. As BSi dissolution is considered to be a controlling factor on Si export, its process description is crucial for the model. Existing models simulate Si originating from BSi by adding biomass fluxes directly (Gérard et al., 2008) or by dissolving chalcedony (Barré et al., 2009). Although dissolution behavior of continental BSi is described by experimental studies (Fraysse et al., 2009), so far BSi dissolution was not simulated for typical soil conditions.

Land cover has also an important impact on the hydrological fluxes (Bosch and Hewlett, 1982; Brown et al., 2005; Dams et al., 2008). Consequently it affects the residence time of soil solutions and thus the Si concentrations (Lucas, 2001). A synthesis of catchments studies

* Corresponding author at: Institut Scientifique du Service Publique, Cellule Risques Sous-sol, Rue du Chéra 200, 4000 Liège, Belgium.
E-mail address: b.ronchi@issep.be (B. Ronchi).

http://dx.doi.org/10.1016/j.geoderma.2017.10.011
Received 16 November 2015; Received in revised form 2 October 2017; Accepted 10 October 2017

(generally under temperate climate conditions but also including some other climates) showed that an increase in tree cover of 10% in forests would decrease the water yield with 25–40 mm and may increase transpiration of water by deep roots up to 50% (Jackson et al., 2000). In contrast, deforestation increases the yield: an increase of 17–19 mm in yield is estimated for a 10% reduction in the cover of deciduous hardwood under temperate and tropical climate conditions (Sahin and Hall, 1996). Simulations for an artificial watershed under temperate climate estimates the evapotranspiration decrease to be about 200 mm.yr^{-1} when forest is replaced by barley (Fohrer et al., 2001).

Given the variety of processes controlling Si export in soils, this paper presents a simple numerical model as a first step to tackle two research questions: (1) how does BSi dissolve in the soil environment; and (2) which impact has a change in water flux on Si export following deforestation?

2. Material and methods

Our approach to simulate kinetic dissolution of biogenic Si in a forest soil followed three steps. Firstly, a kinetic equation was calibrated based on leaching experiments of soil columns at constant water flux. Then, the calibrated equation was used to simulate the Si export from a forest soil under varying atmospheric conditions. Finally, the same model was used to simulate the impact of reduced evapotranspiration due to deforestation and consequently increased soil water fluxes on the Si export. All models were simulated with the HP1 software which couples Hydrus 1D with PhreeqC (Jacques and Simunek, 2005).

2.1. Kinetic BSi dissolution

In order to calibrate the kinetic equation describing BSi dissolution, the soil column tests described in Ronchi et al. (2015) were simulated with the HP1 model (Jacques and Simunek, 2005). The geometry of the model was defined by a column with a length of 6 cm and subdivided into 25 nodes. The water flowing through the column with a flux of 0.8 cm d^{-1} had a pH of 6.83 and Si concentrations of 0.0018 mmol l^{-1}. An initial solution was defined in the column with a pH ($pH_{solution}$) equal to the soil pH (pH_{soil} in Table 1) and Si concentrations equal the final Si concentrations measured in the leached solution ($[Si]_f$ in Table 1).

The highly reactive Si (here hypothesized as just being BSi) dissolution was identified in Ronchi et al. (2015) by the rapid decline in Si concentrations of the leaching curve, characterizing parabolic kinetics. The background concentration, equal to the concentration at the end of the curve, was determined by slow dissolution processes of stable minerals. Since parabolic kinetics are generally described for several silicates with Eq. (1).

$$r = k * t^{-0.61} \quad (1)$$

where r is the weathering rate (mol m^{-2} s^{-1}; White and Brantley, 2003) and t is time (s), we used Eq. (1) to calibrate BSi dissolution in HP1. As pointed out in Ronchi et al. (2015), a proton activity term should also be added in the kinetic equation to account for soil acidity. This term will be tested in the calibration phase.

Table 1
Initial and final concentrations measured in the leached solution from two soils and characteristics of the Luvisol A horizon under forest cover (Af_{lv}) and the Cambisol A horizon under forest cover (Af_{cb}) (Ronchi et al., 2015).

	Af_{cb}	Af_{lv}
$[Si]_i$ (mmol l^{-1})	1.3–1.7	2.1–2.4
$[Si]_f$ (mmol l^{-1})	0.3	0.6
BSi (mg g^{-1})	5	5.4
pH_{soil}	4.1	3.3
$pH_{solution}$	4	3

As we used parabolic kinetics, the calibration only focused on the part of the curve where BSi dissolution was evident: the exponential decline in Si concentrations of the leaching curve (only the first 8 points of the measured curve in Ronchi et al., 2015). Other minerals were not taken into account in this approach. We chose to fit our first numerical model on the Luvisol column (described in Ronchi et al., 2015), as this soil is also used in the next model (Section 2.2), with the lowest measured concentrations in order to simulate minimum concentrations. The model is tested and evaluated on the other Luvisol replica and on the Cambisol columns described in Ronchi et al. (2015).

2.2. Study area

The Meerdaal catchment is located in Central Belgium (Oud-Heverlee, 50°48′1.92″N, 4°40′9.18″O; Fig. 1a). The temperate climate is characterized by a mean temperature of 3.1 °C in January and 17.7 °C in July. During the monitoring period (2010 − 2013), a mean annual precipitation of 590 mm was measured in the forest. Topography varies between 50 and 100 m above sea level. The catchment area spreads over 2.65 km^2 (Fig. 1b–c) and is entirely covered by forest. The deciduous forest is characterized by native beech (*Fagus sylvatica* L) and oak (*Quercus robur* L) (Clymans et al., 2013).

Silty loam soils developed on Late Glacial loess (Deckers et al., 2009), which is underlain by the sandy aquifer of the Brussel Formation and the clayey Kortrijk Formation (Fig. 1c). The mineralogy is principally composed of primary minerals (Quartz, K-feldspar) and clays, e.g. smectite, illite, kaolinite (Vandevenne et al., 2015).

Hydrological fluxes were monitored in this catchment in several studies (Clymans et al., 2013; Van Gaelen et al., 2014). Soil pore water was extracted with suction cups (− 800 hPA) and had mean dissolved Si concentrations of 0.34 ± 0.12 mmol l^{-1} (Van Gaelen et al., 2014). Soil water content was measured monthly with TDR sensors installed next to the suction cups. Groundwater was sampled with a peristaltic pump from three piezometers located near the stream. The piezometer located near the suction cups had the highest groundwater levels (PM1 Fig. 1) and average Si concentrations of 0.24 mmol l^{-1}, typical for the riparian zone according to a PCA (Van Gaelen et al., 2014). The two other piezometers had Si concentration averages around 0.4 mmol l^{-1} (Van Gaelen et al., 2014). As the groundwater sampled in these piezometers would come from beyond the topographical divide (Clymans et al., 2013), its composition resulted from the equilibration of the groundwater with a larger part of the Brussel sand aquifer.

2.3. Modelling of a soil profile

We simulate a soil column comparable with a soil column from the middle of the slope of Meerdaal (around PM1 – Fig. 1c–d) in HP1. The column is 3 m long and divided into 100 nodes and 3 layers with different hydraulic parameters (Table 2). The longitudinal dispersivity was estimated as a tenth of the profile thickness (3 m) based on general correlations between observation scales and longitudinal dispersivities (Gelhar et al., 1992) in saturated porous media. Atmospheric boundary conditions were set at the top of the column, based on precipitation data measured in situ and evapotranspiration data from the station from the Vlaamse Milieu Maatschappij located in Liedekerke (at 40 km from the forest). The simulation is 1802 days long (13/01/2009–19/12/2013), however the first 2 years consist in a 'numerical warming-up' period (13/01/2009–13/01/2011). The input data for the warming-up period is a copy of the data used for the rest of the simulation. At the bottom of the column, the hydraulic boundary condition is set equal to the groundwater level measured in PM1. Root water uptake was not simulated in this model. The first model is called model R. A similar model, R_{-200}, has a decreased evapotranspiration of 200 mm yr^{-1} in order to simulate the Si flux after deforestation, as suggested in Fohrer et al. (2001).

The chemical composition of the influent (Table 3) is based on the

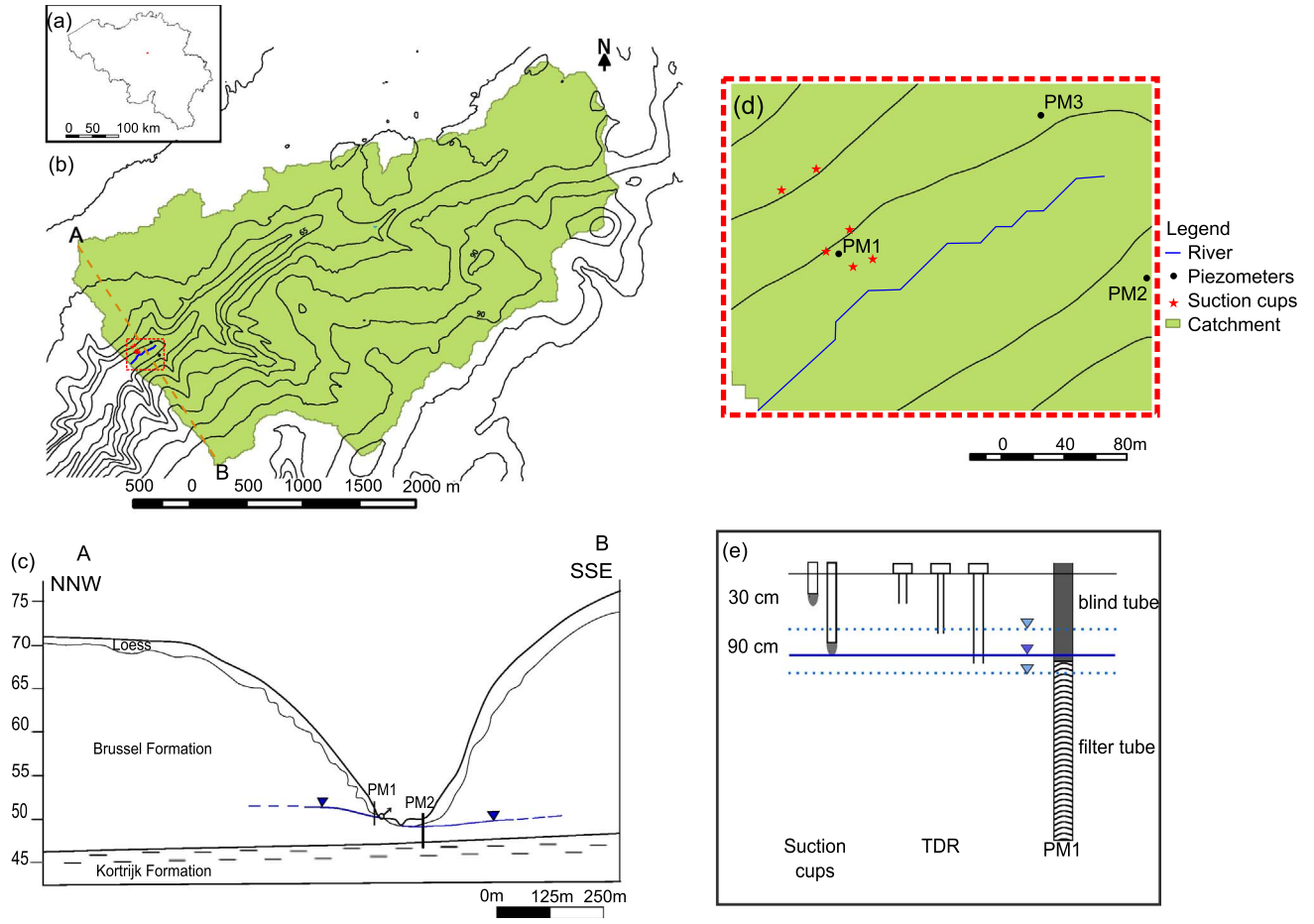

Fig. 1. (a) Location of the catchment; (b) topographic map of the catchment; (c) geological profile through the line A–B from (after Clymans et al., 2013) (b); (d) location of measurements – zoom of red square from (b); (e) setting of suction cups, TDR and piezometer. (For interpretation of the references to colour in this figure legend, the reader is referred to the web version of this article.)

Table 2
Hydraulic parameters of the different layers of the model the residual (θ_r) and saturated (θ_s) water content; saturated hydraulic conductivity (K_s in cm d^{-1}) and the Van Genuchten parameters (α, n, l).

Layer		Depth (cm)	θ_r	θ_s	α	n	K_s (cm d^{-1})	l
1	Humus	0–6	0.1	0.35	0.007	1.6	70	0.21
2	Loam	7–98	0.089	0.35	0.03	1.5	0.8	0.5
3	Sand	99–300	0.065	0.35	0.075	1.89	106.1	0.5

Table 3
Chemical composition (mmol l^{-1}) of rainwater applied to the column. Rain water composition was based on data of Peeters (2010).

	mmol l^{-1}
K	0.0057
Ca	0.0018
Mg	0.005
Na	0.118
SO_4^{2-}	0.0315
Si	0.008
HCO_3^-	0.034733
NO_3^-	0.05407
Cl	0.0149
pH	5.49

rain composition used in a regional model (Peeters, 2010). Based on the model of Barré et al. (2009), we assumed primary minerals as chemically inert or as reacting too slowly compared to BSi and clays. In the first 10 nodes, the kinetic reaction of BSi was applied as BSi was has been identified in this part of the soil column (Vandevenne et al., 2015). The infiltrating solution equilibrated with clay minerals (illite and Ca-montmorillonite) only in the first 2 nodes. This choice was made as simulations with clay equilibration in more nodes took more computing timing but resulted with the same element concentrations. The whole column was undersaturated with respect to CO_2. This reaction was buffered by calcite equilibration in the saturated zone.

3. Results

3.1. Approximation of BSi kinetics

The best fit of Eq. (1) was obtained for Af_{lv2} (Fig. 2) with the following equation:

$$r = (9.0{*}10^{-1} + [H^+]){*}t^{-0.61} \quad (2)$$

The equation simulated the correct range of concentrations for the start of all curves (Fig. 2), but the squared errors were higher for the Cambisol than for the Luvisol (Table 4). For unknown reasons, the shape of curve Af_{cb2} differs completely from Af_{cb1}. Therefore this model does not fit this curve (large squared errors in Table 4). The end of the curve is influenced by pH enhanced weathering of stable minerals and was not simulated in this simplified approach.

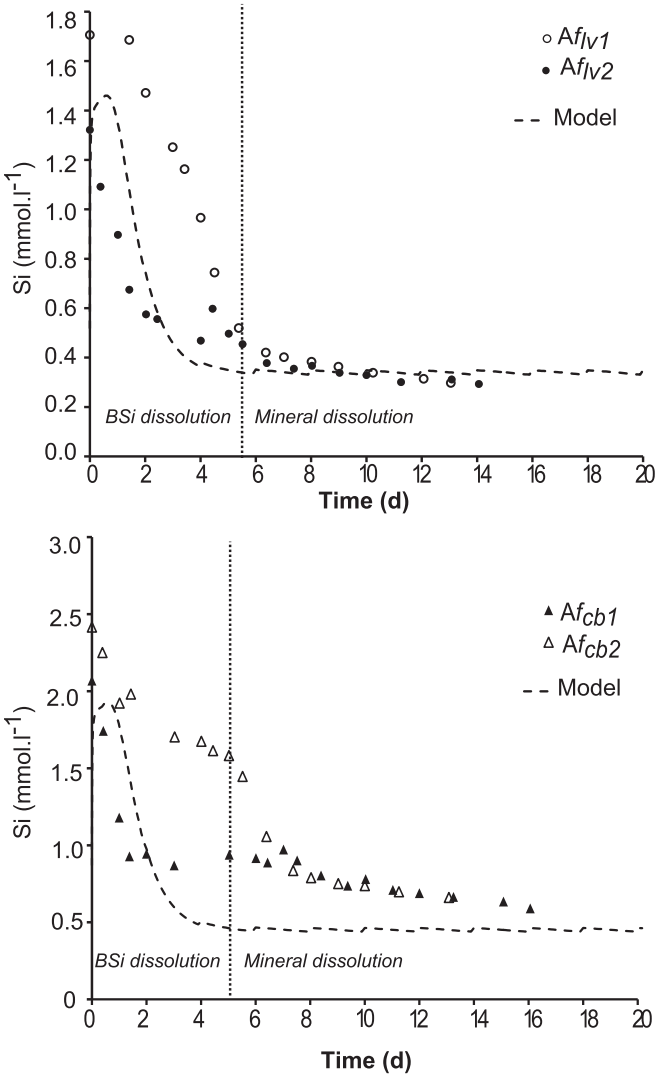

Fig. 2. Si concentrations measured during the column test for the Luvisol (above: Af_{lv}) and Cambisol (below: Af_{cb}) (Ronchi et al., 2015) compared with Si concentrations simulated by the model.

Table 4
Sum of squared errors (SSE), mean squared errors (MSE) and determination coefficient (r^2) for the measured concentrations and simulated concentrations at the start of the curve (8 first measured points corresponding to the dissolution of BSi in Fig. 2). r^{2*} corresponds to the determination coefficient of the same points except the first one.

	SSE	MSE	r^2	r^{2*}
Af_{lv1}	3.98	0.50	0.53	0.73
Af_{lv2}	1.21	0.15	0.15	0.81
Af_{cb1}	2.52	0.31	0.14	0.58
Af_{cb2}	8.02	1.00	0.40	0.83

The coefficients of determination (r^2 in Table 4) were low due to the low concentration simulated by the model at time 0 (0.50 mmol l^{-1} for Af_{cb} and 0.87 mmol l^{-1} for Af_{lv}), not observed in Fig. 2. At the beginning of the calculated curve, values vary a lot, e.g. between 0.050 and 1.4 mmol l^{-1} for Af_{lv}. The first sample taken in the experiment corresponds actually to a mixed sample of the first points of the calculated curve, as enough volume was needed for lab analysis. This explains the important difference between the initial concentrations of the model and the experiment. Coefficients of determination are at least 0.20 units higher when the first point is not taken into account (r^{2*} in Table 4).

3.2. Si concentrations in the soil column models

In both models, Si concentrations were almost constant in time in the deeper part of the column (150 & 222 cm), when water flow conditions were saturated ($h > 0$, Fig. 3). Variation of Si was much more important in time in the upper part of the column (15 & 45 cm depth), under unsaturated conditions ($h < 0$, Fig. 3).

Higher and more variable Si concentrations were calculated in model R (0.32 ± 0.13 mmol l^{-1}) than in model R_{-200} (0.23 ± 0.07 mmol l^{-1}) (Fig. 3). These averages were calculated on the basis of all observation nodes. In contrast, the downward total Si fluxes measured at the bottom of the column after 1802 days of simulation were less important in the R model (-0.119 mol m^{-2}) than in the R_{-200} model (-0.197 mol m^{-2}). This difference was due to the lower yearly evapotranspiration in model R_{-200} creating a higher cumulative bottom flux (0.93 m in R_{-200} vs 0.54 m in R). Pressure heads differed also, i.e. during the months July 2010 and July 2011 pressure heads had lower local minima in R than in R_{-200}.

3.3. Processes controlling Si concentrations in the unsaturated zone

As most variation in Si concentrations was observed in the top of the column, the following analysis focused on the observation node located at 15 cm depth. As expected, none of the tested parameters completely controls the Si concentration as the calculated Pearson correlation coefficients (r; Table 5) are generally much lower than 1. Nevertheless, flux conditions seemed to be the most important factor to control Si concentrations in model R where higher downward fluxes increases Si concentrations ($r = -0.38$ in Table 5). The r-value is negative as downward fluxes were negative in the model, in contrast to upward fluxes created by evapotranspiration. In model R_{-200}, Si concentrations correlated better with hydraulic heads ($r = -0.58$ in Table 5) than with fluxes ($r = -0.42$ in Table 5), Si concentrations are higher when hydraulic heads are negative (like in unsaturated zone). Correlations with the amount of dissolved BSi and the pH were lower (Table 5).

3.4. BSi dissolution

At 15 cm depth, 0.25 mol BSi dissolved during the simulation period in model R. The amount of dissolved BSi correlated with the water flux ($r = -0.48$; Fig. 4). In model R_{-200} only 0.06 mol BSi reacted during the simulation period and correlation with flux was a bit lower ($r = -0.42$; Fig. 4). Si concentrations generally decreased with increasing hydraulic heads (Fig. 5) and were thus generally low during the wet periods (e.g. Fig. 6 above).

At peak flux moments during the wet season, Si concentrations generally decreased due to dilution (e.g. at 10-2-2012 in Fig. 6). In dryer seasons, when pressure heads (h) were low Si concentrations were high (Fig. 5; e.g. June and September 2012 in Fig. 6). Nevertheless, high Si concentrations also occurred at high h (Fig. 5; e.g. 23-5-2012 in Fig. 6). Those peaks were simultaneous with the major dissolved BSi (Δ_{BSi}) peaks. Consequently, the spread of Si concentrations and dissolved BSi was important in saturated conditions ($h = 0$; Fig. 5). The largest dissolved BSi peaks occurred simultaneously with flux peaks following a dry period, i.e. during rewetting events (e.g. 23-5-2012 in Fig. 6).

4. Discussion

4.1. Net Si flux

By simulating the equilibration of clay minerals and the kinetic dissolution of BSi in the top soils, average Si concentration in the R model (0.32 mmol l^{-1} - Table 6) were close to the mean concentrations measured in Meerdaal forest (0.34 ± 0.12 mmol l^{-1}; Van Gaelen et al., 2014). The average Si concentration simulated in the soil pore

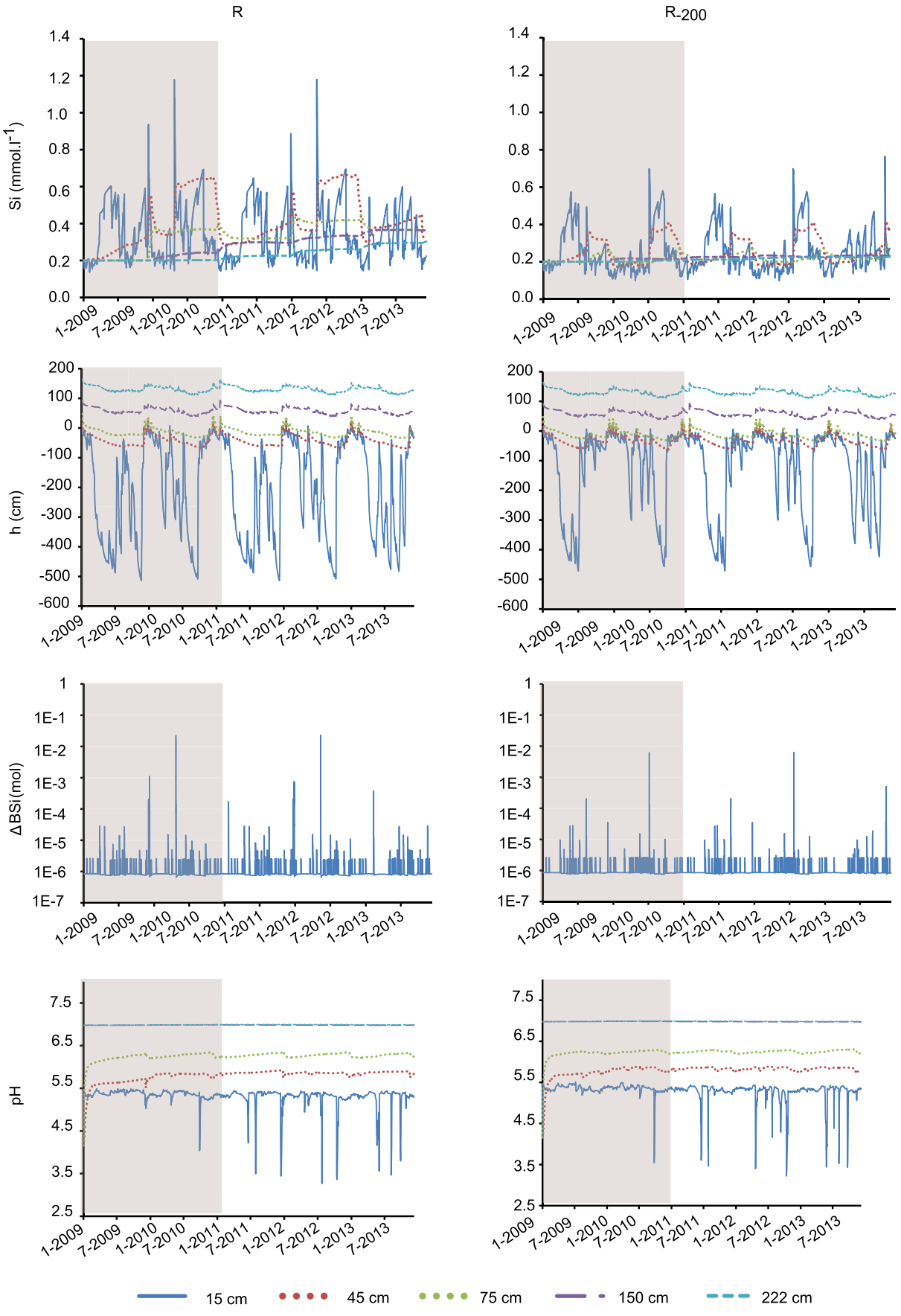

Fig. 3. Variation in time of simulated Si concentrations (mmol l^{-1}), pressure heads (h in cm), amount of kinetically reacted BSi (Δ_{BSi} in mol) and pH at different depths in the simulated column (15, 45, 75, 150, 222 cm) for the both models R and R_{-200}. The shaded area represents the warm-up period.

Table 5
Pearson correlation coefficients (r) calculated between Si concentrations at 15 cm and pH, dissolved BSi (Δ_{BSi}), hydraulic heads (h), soil water content (Θ) and flux for the models *R* and R_{-200}. Bold values indicate the highest correlations.

	R	R_{-200}
pH	− 0.09	− 0.07
Δ_{BSi}	0.17	0.14
h	− 0.29	**− 0.58**
Θ	− 0.07	− 0.42
Flux	**− 0.38**	− 0.13

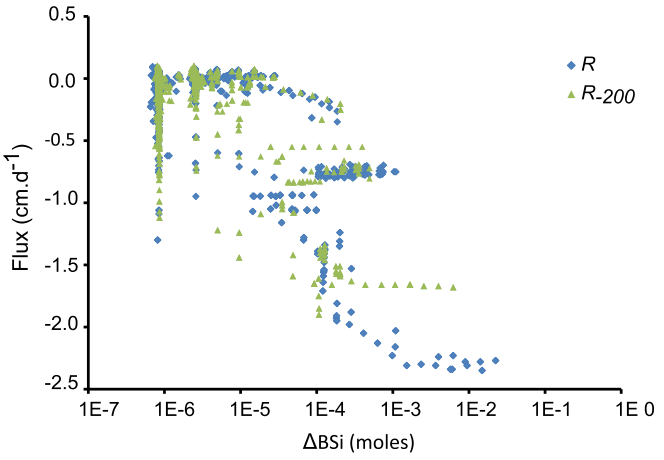

Fig. 4. Correlation between the flux and the amount of dissolved BSi calculated for daily time steps by the models *R* (diamonds) and the model R_{-200} (triangles).

water of the "early deforested soil" simulated in model R_{-200} was lower (0.23 mmol l^{-1}- Table 6). This difference can be partially explained by the higher amount of BSi that dissolved in model *R* ($F\Delta_{BSi}$ in Table 6 –0.051 mol m^{-2} yr^{-1}). A similar Si flux (0.053 mol m^{-2} yr^{-1}) due to BSi dissolution was estimated for a forest soil by Gérard et al. (2008). White et al. (2012) estimated a higher Si flux (0.065 mol m^{-2} yr^{-1}) coming from a readily soluble Si pool (extracted with an alkaline solution) in grassland, but this pool not only took into account BSi but also amorphous pedogenic Si.

In contrast, the yearly Si flux delivered by the column was higher in model R_{-200} (0.040 mol m^{-2} yr^{-1}) than in model *R* (0.024 mol m^{-2} yr^{-1}-F_{Si} in Table 6). These were higher but in the same order of magnitude as the Si discharge calculated in previous studies for grasslands (0.018 mol m^{-2} yr^{-1} in White et al., 2012) and forests (0.018 mol m^{-2} yr^{-1} in Gérard et al., 2008). The difference can be attributed to the fact that our model did not simulate uptake by plants and that no mineral precipitation was considered.

Our models simulated the highest Si concentrations in the unsaturated zone. Water fluxes were an important controlling factor for Si concentrations, especially in the *R* models (Table 5). By comparing the two models, we observe that higher fluxes (R_{-200}) resulted in lower Si concentrations. Moreover, at the scale of a rain event during the wet season, we observe that Si concentrations (R_{-200}) decreased (Fig. 5). This dilution effect was due to the low residence time which did not allow pore water to reach equilibrium (Maher, 2011). Such dilution processes were also observed in the study of Si concentrations in the river where fresh DSi-poor soil water fed the river during rain events (Clymans et al., 2013). In contrast, the model with lower cumulative fluxes (FSi in Table 6), i.e. *R*, delivered higher Si concentrations as larger amounts of biogenic Si (Δ_{BSi}) could react. During rewetting conditions in the dry season, peaks of the kinetic BSi dissolution were observed.

The low Si concentrations in soil water of R_{-200} did not correspond to the increase in DSi concentrations measured in rivers of the Hubbard

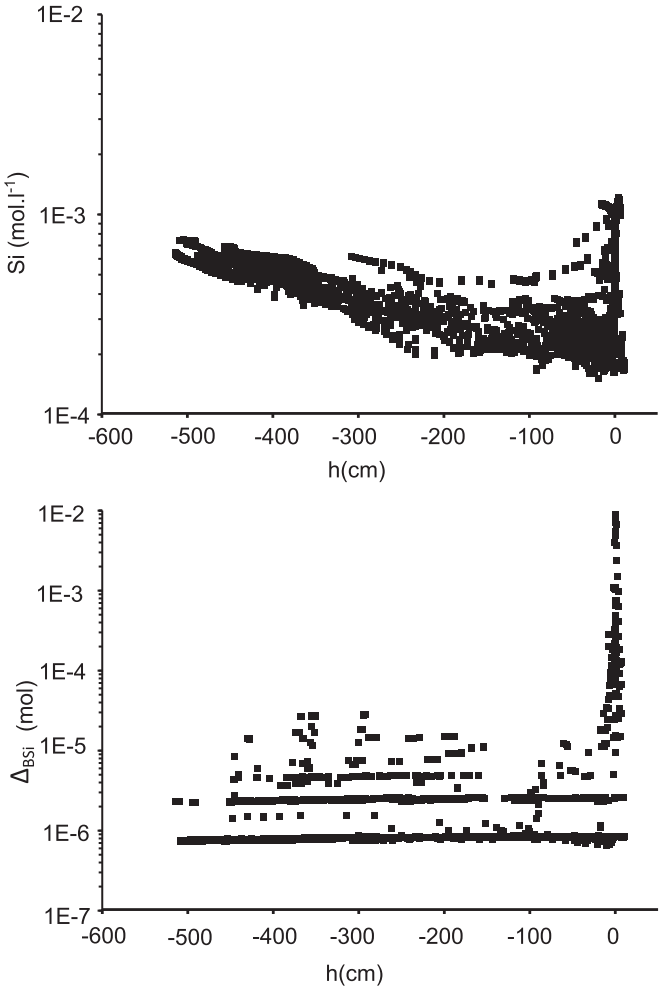

Fig. 5. Si concentrations (mol l^{-1}) and amounts dissolved BSi (Δ_{BSi}) calculated for daily time steps, plotted against pressure heads (h in cm) at 15 cm depth in model *R*. Similar trends were observed for the other model.

Brook Experimental forest after deforestation (Conley et al., 2008). However, different processes are observed in each case. In the Hubbard Brook Experimental forest, BSi eroded from the upper soil horizon was transported as particles to the river, where it subsequently dissolved and provided higher Si concentrations in the river. This does not apply in our model where the dissolution of Si takes place in the soil.

4.2. Model uncertainties

Our model is the first simulation of dissolved Si export from forest soils taking into account the kinetic reactions of BSi. We choose to use a simple kinetic approach that approximated our experimental curves. As in the experimental curves some internal variation occurred, our equation should also be tested on larger datasets to assess the uncertainty on the fitted equation.

The model considering variable atmospheric boundary conditions and clay equilibration reproduced comparable water content and Si concentration ranges as measured in the field with this kinetic equation. However it did not reproduce exact time series since it was not calibrated for water fluxes. Therefore, our analysis focused on the understanding of BSi dissolution and less on absolute quantification of an entire Si cycle. It is a simplified view of a complex system where soil water chemistry is dependent on bedrock composition, topography, drainage conditions, rainfall distribution throughout the year and plant uptake. Nutrient uptake was not taken into account in this model as convergence problems occurred when this was included in the model. It

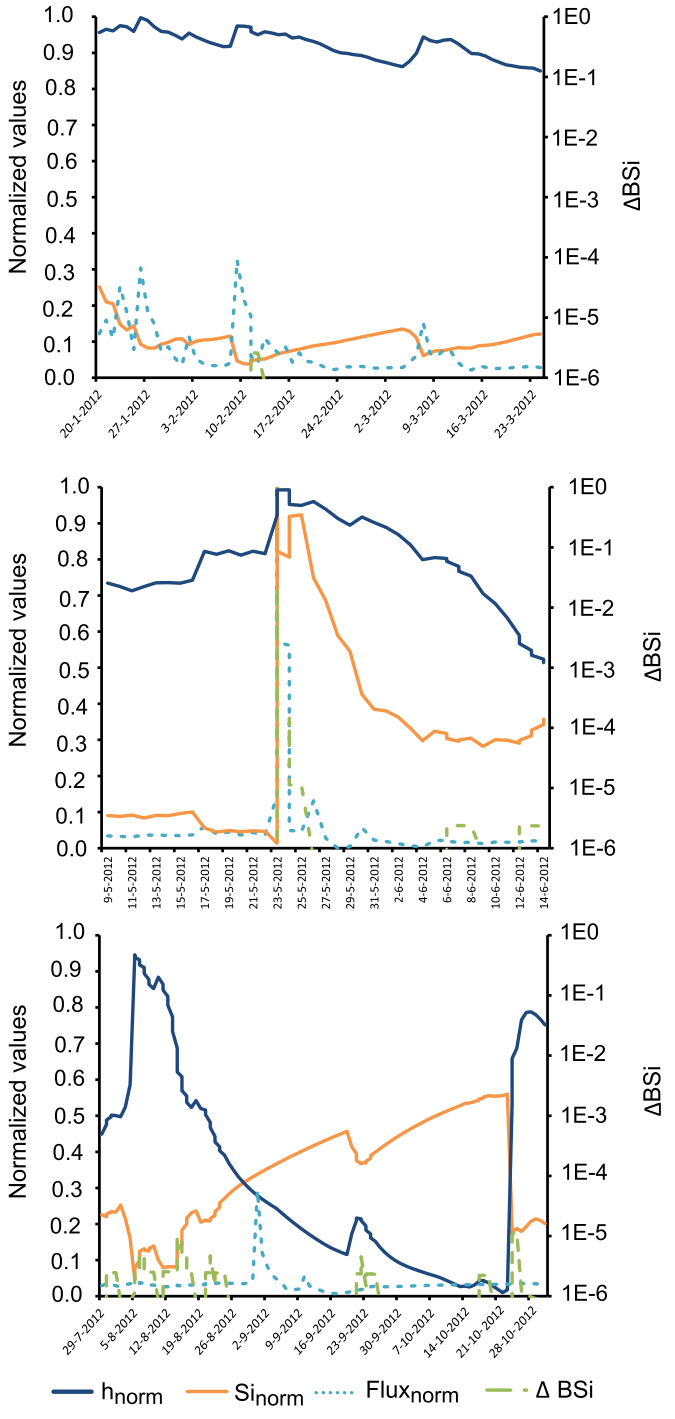

Fig. 6. Normalized Si concentrations, pressure heads (h), flux (left axe) and the amount of kinetically dissolved BSi (right axe) in the wet season (above) and dry season (middle and below) of the year 2012 in model *R* at 15 cm depth. Normalization facilitates the comparison between the different variables. To plot intense flux as a positive peak, signs of fluxes were inversed for normalization: positive flux is in this figure downward flux. Dissolved BSi amounts are plotted logarithmically (right axe).

would however be interesting to develop the model to verify if the Si uptake and release by the forest biomass are (nearly) equal (Alexandre et al., 1997; Sommer et al., 2012).

In further developments of the model, processes linked to weathering minerals should be integrated in the model. This is needed to fully understand the Si cycle in the soil as clays can incorporate dissolved Si from phytoliths (Cornelis et al., 2014a) or release DSi in organic rich environments (Cardinal et al., 2010; Cornelis et al., 2010). Including other nutrient cycles would allow estimates of CO_2 consumption by weathering processes (Goddéris et al., 2006), better estimations of K concentrations (Goddéris et al., 2006) and a better understanding of the influence of the presence of forest (vs a deforested soil) on the weathering processes. To integrate these aspects in such models, large ranges of solubility of different clay minerals (Violette et al., 2010) should be tested as thermodynamic databases are based on experimental observations on pure clays, and not on interstratified soil clays. Also the chemistry of throughfall, the primary production of plants (Barré et al., 2009) and the cation exchange capacity of clays (Goddéris et al., 2006) should be integrated. In further developments of this model, not only the sensitivity of these parameters should be tested but also the role of clays in the Si cycle should be better constrained. Unlike the WITCH model of Goddéris et al. (2006), the cation exchange capacity of clays was not simulated in this model. This affects the availability of cations for plants but also for clay formation. If these aspects are simulated in future models, the model results will not only focus on Si export but also on cation export.

Table 6
Summary of the model results. Average Si concentrations and standard deviations for all observation nodes (15, 45, 75, 150, 222 cm); yearly water outflux of the column (*F*) calculated from the cumulative bottom flux; the yearly Si flux at the bottom of the column (F_{Si}); the yearly Si flux originating from the kinetical dissolution of BSi ($F\Delta_{BSi}$) at 15 cm depth; and the average pH with the standard deviation calculated at 15 cm. In brackets, the minimum value calculated for the pH at 15 cm depth.

	R	R_{-200}
[Si] (mmol l^{-1})	0.32 ± 0.13	0.23 ± 0.07
F (m yr^{-1})	0.11	0.19
F_{Si} (mol m^{-2} yr^{-1})	0.024	0.040
$F\Delta_{BSi}$ (mol m^{-2} yr^{-1})	0.051	0.013
pH	5.30 ± 0.24 (3.27)	5.28 ± 0.26 (3.23)

5. Conclusion

The estimation of a kinetic equation simulating BSi dissolution allowed the prediction of dissolved Si concentrations in soil water close to field values, and gave Si fluxes due to BSi dissolution close to what was found in other studies (Gérard et al., 2008; White et al., 2012). This equation should thus be tested on larger datasets and applied in other models concerning Si cycles or weathering processes.

From our models it was clear that not only BSi dissolution but that also the water flux controlled Si export. After deforestation, the water flux increases, due to a transpiration decrease, diminishing the overall amount of dissolved BSi and Si concentrations in the soil water. BSi dissolution under forest is thus favored by the lower fluxes. Nevertheless the total exported DSi flux was higher under the deforested soil.

Applying such models for soils covered by different land use types (and in different climatic conditions) at catchment scale would improve the understanding of continental Si export to the hydrographic system. In the model of Laruelle et al. (2009), one global average DSi concentration of 0.2 mmol l^{-1} is used for the terrestrial DSi reservoir. Other models integrated the impact of land use change on Si export by taking into account changes in suspended Si material but neglected the influence on DSi (Dürr et al., 2011). Our simulations prove that for global models, the spatial hetereogeneity of continental Si cycling would better be estimated after the development of catchment scale models taking hydrological conditions and kinetic BSi dissolution into account. It would improve the understanding of the impact of human activities on weathering and pedogenic processes.

Acknowledgements

B. Ronchi would like to thank the Flemish Agency for the promotion

of Innovation by Science and Technology (IWT) for providing a PhD grant. Prof. Jan Diels, Prof. Gerard Govers, Prof. Jan Elsen, Prof. Sophie Opfergelt and Prof. Daniel Conley and the reviewers are thanked for their critical remarks on an earlier version of this manuscript.

References

Alexandre, A., Meunier, J.-D., Colin, F., Koud, J.-M., 1997. Plant impact on the biogeochemical cycle of silicon and related weathering processes. Geochim. Cosmochim. Ac. 61, 677–682. http://dx.doi.org/10.1016/S0016-7037(97)00001-X.

Barré, P., Berger, G., Velde, B., 2009. How element translocation by plants may stabilize illitic clays in the surface of temperate soils. Geoderma 151, 22–30. http://dx.doi.org/10.1016/j.geoderma.2009.03.004.

Bosch, J.M., Hewlett, J.D., 1982. A review of catchment experiments to determine the effect of vegetation changes on water yield and evapotranspiration. J. Hydrol. 55 (1–4), 3–23.

Brown, A.E., Zhang, L., McMahon, T.A., Western, A.W., Vertessy, R.A., 2005. A review of paired catchment studies for determining changes in water yield resulting from alterations in vegetation. J. Hydrol. 310, 28–61.

Cardinal, D., Gaillardet, J., Hughes, H.J., Opfergelt, S., André, L., 2010. Contrasting silicon isotope signatures in rivers from the Congo Basin and the specific behaviour of organic-rich waters. Geophys. Res. Lett. 37 n/a–n/a. https://doi.org/10.1029/2010GL043413.

Carey, J.C., Fulweiler, R.W., 2011. Human activities directly alter watershed dissolved silica fluxes. Biogeochemistry. http://dx.doi.org/10.1007/s10533-011-9671-2.

Carey, J.C., Fulweiler, R.W., 2013. Watershed land use alters riverine silica cycling. Biogeochemistry 113, 525–544. http://dx.doi.org/10.1007/s10533-012-9784-2.

Clymans, W., Struyf, E., Govers, G., Vandevenne, F., Conley, D.J., 2011. Anthropogenic impact on biogenic Si pools in temperate soils. Biogeosci. Discuss. 8, 4391–4419. http://dx.doi.org/10.5194/bgd-8-4391-2011.

Clymans, W., Govers, G., Frot, E., Ronchi, B., Van Wesemael, B., Struyf, E., 2013. Temporal dynamics of bio-available Si fluxes in a temperate forested catchment (Meerdaal forest, Belgium). Biogeochemistry. http://dx.doi.org/10.1007/s10533-013-9858-9.

Conley, D.J., Likens, G.E., Buso, D.C., Saccone, L., Bailey, S.W., Johnson, C.E., 2008. Deforestation causes increased dissolved silicate losses in the Hubbard brook experimental Forest. Glob. Chang. Biol. 1–7. http://dx.doi.org/10.1111/j.1365-2486.2008.01667.x.

Cornelis, J.-T., Delvaux, B., Cardinal, D., André, L., Ranger, J., Opfergelt, S., 2010. Tracing mechanisms controlling the release of dissolved silicon in forest soil solutions using Si isotopes and Ge/Si ratios. Geochim. Cosmochim. Ac. 74, 3913–3924. http://dx.doi.org/10.1016/j.gca.2010.04.056.

Cornelis, J.-T., Dumon, M., Tolossa, A.R., Tolossa, A.R., Delvaux, B., Deckers, J., Van Ranst, E., 2014. The effect of pedological conditions on the sources and sinks of silicon in the Vertic Planosols in South-western Ethiopia. Catena 112, 131–138. http://dx.doi.org/10.1016/j.catena.2013.02.014.

Dams, J., Woldeamlak, S.T., Batelaan, O., 2008. Predicting land-use change and its impact on the groundwater system of the Kleine Nete catchment, Belgium. Hydrol. Earth Syst. Sci. 12, 1369–1385. http://dx.doi.org/10.5194/hess-12-1369-2008.

Deckers, J., Langohr, R., Poesen, J., Vancampenhout, K., 2009. Natuur en cultuur volgens de bodem. In: De Bie, H., Hermy, M., Van den Bremt, P. (Eds.), Miradal. Erfgoed Heverleebos en Meerdaalwoud. Davidsfonds, Leuven, Belgium, pp. 34–45.

Dürr, H.H., Meybeck, M., Hartmann, J., Laruelle, G.G., Roubeix, V., 2011. Global spatial distribution of natural riverine silica inputs to the coastal zone. Biogeosciences 8, 597–620.

Epstein, E., 1999. Silicon. Annu. Rev. Plant Physiol. Plant Mol. Biol. 50, 641–664. http://dx.doi.org/10.1146/annurev.arplant.50.1.641.

Farmer, V.C., Delbos, E., Miller, J.D., 2005. The role of phytolith formation and dissolution in controlling concentrations of silica in soil solutions and streams. Geoderma 127, 71–79. http://dx.doi.org/10.1016/j.geoderma.2004.11.014.

Fohrer, N., Haverkamp, S., Eckhardt, K., Frede, H.-G., 2001. Hydrologic response to land use changes on the catchment scale. Phys. Chem. Earth, Part B Hydrol. Ocean Atmos. 26, 577–582. http://dx.doi.org/10.1016/S1464-1909(01)00052-1.

Fraysse, F., Pokrovsky, O.S., Schott, J., Meunier, J.-D., 2009. Surface chemistry and reactivity of plant phytoliths in aqueous solutions. Chem. Geol. 258, 197–206. http://dx.doi.org/10.1016/j.chemgeo.2008.10.003.

Fulweiler, R.W., Nixon, S.W., 2005. Terrestrial vegetation and the seasonal cycle of dissolved silica in a southern New England coastal river. Biogeochemistry 74, 115–130. http://dx.doi.org/10.1007/s10533-004-2947-z.

Gelhar, L.W., Welty, C., Rehfeldt, K., 1992. A critical review of data on field-scale dispersion in aquifers. Water Resour. Res. 28, 1955–1974.

Gérard, F., François, M., Ranger, J., 2002. Processes controlling silica concentration in leaching and capillary soil solutions of an acidic brown forest soil (Rhône, France). Geoderma 107, 197–226.

Gérard, F., Mayer, K.U., Hodson, M.J., Ranger, J., 2008. Modelling the biogeochemical cycle of silicon in soils: application to a temperate forest ecosystem. Geochim. Cosmochim. Acta 72, 741–758. http://dx.doi.org/10.1016/j.gca.2007.11.010.

Goddéris, Y., François, L.M., Probst, A., Schott, J., Moncoulon, D., Labat, D., Viville, D., 2006. Modelling weathering processes at the catchment scale: the WITCH numerical model. Geochim. Cosmochim. Acta 70, 1128–1147.

Jackson, R.B., Schenk, H., Jobbagy, E.G., Canadell, J., Colello, G.D., Dickinson, R.E., Field, C.B., Friedlingstein, P., Heimann, M., Hibbard, K., Kicklighter, D.W., Kleidon, A., Neilson, R.P., Parton, W.J., Sala, O.E., Sykes, M.T., 2000. Belowground consequences of vegetation change and their treatment in models. Ecol. Appl. 10, 470–483.

Jacques, D., Simunek, J., 2005. User Manual of the Multicomponent Variably-Saturated Flow and Transport Model HP1. SCK CEN, Mol, Belgium. http://www.pc-progress.com/Documents/hp1.pdf.

Keller, C., Guntzer, F., Barboni, D., Labreuche, J., Meunier, J.-D., 2012. Impact of agriculture on the Si biogeochemical cycle: input from phytolith studies. Compt. Rendus Geosci. http://dx.doi.org/10.1016/j.crte.2012.10.004.

Laruelle, G.G., Roubeix, V., Sferratore, A., Brodherr, Ciuffa, D., Conley, D.J., Dürr, H.H., Garnier, J., Lancelot, C., Le Thi Phuong, Q., Meunier, J.-D., Meybeck, M., Michalopoulos, P., Moriceau, B., Ni´ Longphuirt, S., Loucaides, S., Papush, L., Presti, M., Ragueneau, O., Regnier, P., Saccone, L., Slomp, C.P., Spiteri, C., Van Cappellen, P., 2009. Anthropogenic perturbations of the silicon cycle at the global scale: key role of the land-ocean transition. Glob. Biogeochem. Cycles 23, GB4031. http://dx.doi.org/10.1029/2008GB003267.

Lucas, Y., 2001. The role of plants in controlling rates and products of weathering: importance of biological pumping. Annu. Rev. Earth Planet. Sci. 29, 135–163.

Maher, K., 2011. The role of fluid residence time and topographic scales in determining chemical fluxes from landscapes. Earth Planet. Sci. Lett. 312, 48–58. http://dx.doi.org/10.1016/j.epsl.2011.09.040.

Peeters, L., 2010. Groundwater and Geochemical Modelling of the Unconfined Brussels Aquifer. Belgium, KULeuven.

Raven, J.A., 2003. Cycling silicon — the role of accumulation in plants. New Phytol. 158, 419–421. http://dx.doi.org/10.1046/j.1469-8137.2003.00778.x.

Ronchi, B., Barão, A.L., Clymans, W., Vandevenne, F., Batelaan, O., Govers, G., Struyf, E., Dassargues, A., 2015. Factors controlling Si export from soils: a soil column approach. Catena 133, 85–96.

Sahin, V., Hall, M.J., 1996. The effects of afforestation and deforestation on water yields. J. Hydrol. 178, 293–309. http://dx.doi.org/10.1016/0022-1694(95)02825-0.

Sommer, M., Jochheim, H., Höhn, A., Breuer, J., Zagorski, Z., Busse, J., Barkusky, D., Puppe, D., Wanner, M., Kaczorek, D., 2012. Si cycling in a forest biogeosystem — the importance of anthropogenic perturbation and induced transient state of biogenic Si pools. Biogeosci. Discuss. 9, 18865–18906. http://dx.doi.org/10.5194/bgd-9-18865-2012.

Struyf, E., Smis, A., Van Damme, S., Garnier, J., Govers, G., Van Wesemael, B., Conley, D.J., Batelaan, O., Frot, E., Clymans, W., Vandevenne, F., Lancelot, C., Goos, P., Meire, P., 2010. Historical land use change has lowered terrestrial silica mobilization. Nat. Commun. 1, 129. http://dx.doi.org/10.1038/ncomms1128.

Tréguer, P.J., De La Rocha, C.L., 2013. The world ocean silica cycle. Annu. Rev. Mar. Sci. 1–25. http://dx.doi.org/10.1146/annurev-marine-121211-172346.

Van Gaelen, N., Verheyen, D., Ronchi, B., Struyf, E., Govers, G., Vanderborght, J., Diels, J., 2014. Identifying the transport pathways of Dissolved Organic Carbon in contrasting catchments. Vadose Zo J 13:-.

Vandevenne, F., Barão, A.L., Ronchi, B., Govers, G., Meire, P., Kelly, E.F., Struyf, E., 2015. Silicon pools in human impacted soils of temperate zones. Glob. Biogeochem. Cycles 29 (9), 1439–1450. http://dx.doi.org/10.1002/2014GB005049.

Violette, A., Goddéris, Y., Maréchal, J.-C., Riotte, J., Oliva, P., Mohan Kumar, M.S., Sekhar, M., Braun, J.-J., 2010. Modelling the chemical weathering fluxes at the watershed scale in the tropics (Mule Hole, South India): relative contribution of the smectite/kaolinite assemblage versus primary minerals. Chem. Geol. 277, 42–60. http://dx.doi.org/10.1016/j.chemgeo.2010.07.009.

White, A.F., Brantley, S.L., 2003. The effect of time on the weathering of silicate minerals: why do weathering rates differ in the laboratory and field? Chem. Geol. 202, 479–506. http://dx.doi.org/10.1016/j.chemgeo.2003.03.001.

White, A.F., Vivit, D.V., Schulz, M.S., Bullen, T.D., Evett, R.R., Aagarwal, J., 2012. Biogenic and pedogenic controls on Si distributions and cycling in grasslands of the Santa Cruz soil chronosequence, California. Geochim. Cosmochim. Acta 94, 72–94. http://dx.doi.org/10.1016/j.gca.2012.06.009.